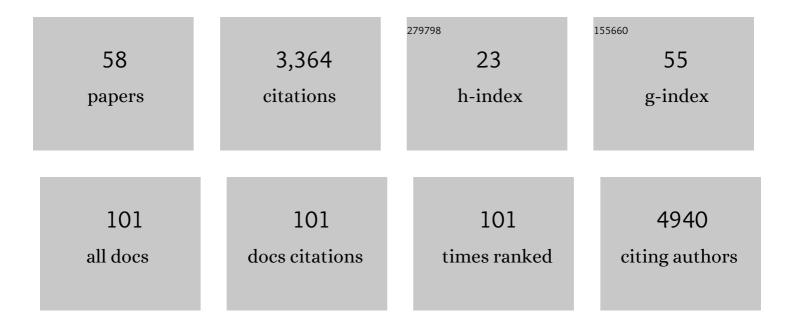
Qiong Zhang

List of Publications by Year in descending order

Source: https://exaly.com/author-pdf/6767949/publications.pdf Version: 2024-02-01



Οιονς Ζηλής

#	Article	IF	CITATIONS
1	Summary of a workshop on extreme weather events in a warming world organized by the Royal Swedish Academy of Sciences. Tellus, Series B: Chemical and Physical Meteorology, 2022, 72, 1794236.	1.6	11
2	Past terrestrial hydroclimate sensitivity controlled by Earth system feedbacks. Nature Communications, 2022, 13, 1306.	12.8	28
3	ECâ€Earth Simulations Reveal Enhanced Interâ€Hemispheric Thermal Contrast During the Last Interglacial Further Intensified the Indian Monsoon. Geophysical Research Letters, 2022, 49, .	4.0	5
4	The EC-Earth3 Earth system model for the Coupled Model Intercomparison Project 6. Geoscientific Model Development, 2022, 15, 2973-3020.	3.6	192
5	Mid-Holocene European climate revisited: New high-resolution regional climate model simulations using pollen-based land-cover. Quaternary Science Reviews, 2022, 281, 107431.	3.0	18
6	Calendar effects on surface air temperature and precipitation based on model-ensemble equilibrium and transient simulations from PMIP4 and PACMEDY. Climate of the Past, 2022, 18, 1047-1070.	3.4	8
7	Northward migration of the East Asian summer monsoon northern boundary during the twenty-first century. Scientific Reports, 2022, 12, .	3.3	8
8	The modulation of westerliesâ€monsoon interaction on climate over the monsoon boundary zone in East Asia. International Journal of Climatology, 2021, 41, E3049.	3.5	21
9	Impacts of Large cale Sahara Solar Farms on Global Climate and Vegetation Cover. Geophysical Research Letters, 2021, 48, e2020GL090789.	4.0	27
10	Simulating the mid-Holocene, last interglacial and mid-Pliocene climate with EC-Earth3-LR. Geoscientific Model Development, 2021, 14, 1147-1169.	3.6	32
11	Understanding the variability of the rainfall dipole in West Africa using the EC-Earth last millennium simulation. Climate Dynamics, 2021, 57, 93-107.	3.8	16
12	Mid-Pliocene Atlantic Meridional Overturning Circulation simulated in PlioMIP2. Climate of the Past, 2021, 17, 529-543.	3.4	20
13	Reconstructing Past Global Vegetation With Random Forest Machine Learning, Sacrificing the Dynamic Response for Robust Results. Journal of Advances in Modeling Earth Systems, 2021, 13, e2020MS002200.	3.8	9
14	Glacio-Nival Regime Creates Complex Relationships between Discharge and Climatic Trends of Zackenberg River, Greenland (1996–2019). Climate, 2021, 9, 59.	2.8	3
15	Regional and Local Impacts of the ENSO and IOD Events of 2015 and 2016 on the Indian Summer Monsoon—A Bhutan Case Study. Atmosphere, 2021, 12, 954.	2.3	10
16	Mid-Pliocene West African Monsoon rainfall as simulated in the PlioMIP2 ensemble. Climate of the Past, 2021, 17, 1777-1794.	3.4	10
17	Mass Balance Sensitivity and Future Projections of Rabots Glaciä Sweden. Climate, 2021, 9, 126.	2.8	3
18	Northwestward shift of the northern boundary of the East Asian summer monsoon during the mid-Holocene caused by orbital forcing and vegetation feedbacks. Quaternary Science Reviews, 2021, 268, 107136.	3.0	23

QIONG ZHANG

#	Article	IF	CITATIONS
19	A multi-model CMIP6-PMIP4 study of Arctic sea ice at 127 ka: sea ice data compilation and model differences. Climate of the Past, 2021, 17, 37-62.	3.4	29
20	Large-scale features of Last Interglacial climate: results from evaluating the <i>lig127k</i> simulations for the Coupled Model Intercomparison Project (CMIP6)–Paleoclimate Modeling Intercomparison Project (PMIP4). Climate of the Past, 2021, 17, 63-94.	3.4	76
21	Reduced El Niño variability in the mid-Pliocene according to the PlioMIP2 ensemble. Climate of the Past, 2021, 17, 2427-2450.	3.4	10
22	Evaluating the large-scale hydrological cycle response within the Pliocene Model Intercomparison Project Phase 2 (PlioMIP2) ensemble. Climate of the Past, 2021, 17, 2537-2558.	3.4	21
23	Northward extension of the East Asian summer monsoon during the mid-Holocene. Global and Planetary Change, 2020, 184, 103046.	3.5	31
24	Drier tropical and subtropical Southern Hemisphere in the mid-Pliocene Warm Period. Scientific Reports, 2020, 10, 13458.	3.3	25
25	Global River Discharge and Floods in the Warmer Climate of the Last Interglacial. Geophysical Research Letters, 2020, 47, e2020GL089375.	4.0	18
26	Origin of the spatial consistency of summer precipitation variability between the Mongolian Plateau and the mid-latitude East Asian summer monsoon region. Science China Earth Sciences, 2020, 63, 1199-1208.	5.2	15
27	The changes in ENSO-induced tropical Pacific precipitation variability in the past warm and cold climates from the EC-Earth simulations. Climate Dynamics, 2020, 55, 503-519.	3.8	8
28	Using the climate feedback response analysis method to quantify climate feedbacks in the middle atmosphere. Atmospheric Chemistry and Physics, 2020, 20, 12409-12430.	4.9	2
29	A Bayesian framework for emergent constraints: case studies of climate sensitivity with PMIP. Climate of the Past, 2020, 16, 1715-1735.	3.4	17
30	Comparison of past and future simulations of ENSO in CMIP5/PMIP3 and CMIP6/PMIP4 models. Climate of the Past, 2020, 16, 1777-1805.	3.4	56
31	Large-scale features and evaluation of the PMIP4-CMIP6 <i>midHolocene</i> simulations. Climate of the Past, 2020, 16, 1847-1872.	3.4	94
32	The Pliocene Model Intercomparison Project Phase 2: large-scale climate features and climate sensitivity. Climate of the Past, 2020, 16, 2095-2123.	3.4	93
33	Evaluation of Arctic warming in mid-Pliocene climate simulations. Climate of the Past, 2020, 16, 2325-2341.	3.4	21
34	Vegetation Pattern and Terrestrial Carbon Variation in Past Warm and Cold Climates. Geophysical Research Letters, 2019, 46, 8133-8143.	4.0	13
35	Northern Hemisphere Land Monsoon Precipitation Increased by the Green Sahara During Middle Holocene. Geophysical Research Letters, 2019, 46, 9870-9879.	4.0	30
36	Thermodynamic and dynamic effects of increased moisture sources over the Tropical Indian Ocean in recent decades. Climate Dynamics, 2019, 53, 7081-7096.	3.8	11

QIONG ZHANG

#	Article	IF	CITATIONS
37	The SPARC water vapour assessmentÂll: profile-to-profile and climatological comparisons of stratospheric <i>Î </i> D(H ₂ O) observations from satellite. Atmospheric Chemistry and Physics, 2019, 19, 2497-2526.	4.9	1
38	Century-scale temperature variability and onset of industrial-era warming in the Eastern Tibetan Plateau. Climate Dynamics, 2019, 53, 4569-4590.	3.8	13
39	Contribution of sea ice albedo and insulation effects to Arctic amplification in the EC-Earth Pliocene simulation. Climate of the Past, 2019, 15, 291-305.	3.4	23
40	The water cycle of the midâ€Holocene West African monsoon: The role of vegetation and dust emission changes. International Journal of Climatology, 2019, 39, 1927-1939.	3.5	18
41	Agreement between reconstructed and modeled boreal precipitation of the Last Interglacial. Science Advances, 2019, 5, eaax7047.	10.3	46
42	Hydroclimate in the Pamirs Was Driven by Changes in Precipitationâ€Evaporation Seasonality Since the Last Glacial Period. Geophysical Research Letters, 2019, 46, 13972-13983.	4.0	31
43	The PMIP4 contribution to CMIP6 – Part 1: Overview and over-arching analysis plan. Geoscientific Model Development, 2018, 11, 1033-1057.	3.6	164
44	Historical (1750–2014) anthropogenic emissions of reactive gases and aerosols from the Community Emissions Data System (CEDS). Geoscientific Model Development, 2018, 11, 369-408.	3.6	1,058
45	Representation of Multidecadal Sahel Rainfall Variability in 20th Century Reanalyses. Scientific Reports, 2018, 8, 10937.	3.3	21
46	Estimation of the maximum annual number of North Atlantic tropical cyclones using climate models. Science Advances, 2018, 4, eaat6509.	10.3	18
47	Dynamic Vegetation Simulations of the Midâ€Holocene Green Sahara. Geophysical Research Letters, 2018, 45, 8294-8303.	4.0	27
48	Understanding the Mechanisms behind the Northward Extension of the West African Monsoon during the Mid-Holocene. Journal of Climate, 2017, 30, 7621-7642.	3.2	32
49	Tropical cyclone activity enhanced by Sahara greening and reduced dust emissions during the African Humid Period. Proceedings of the National Academy of Sciences of the United States of America, 2017, 114, 6221-6226.	7.1	39
50	Greening of the Sahara suppressed ENSO activity during the mid-Holocene. Nature Communications, 2017, 8, 16020.	12.8	63
51	The PMIP4 contribution to CMIP6 – Part 4: Scientific objectives and experimental design of the PMIP4-CMIP6 Last Glacial Maximum experiments and PMIP4 sensitivity experiments. Geoscientific Model Development, 2017, 10, 4035-4055.	3.6	137
52	On the importance of the albedo parameterization for the mass balance of the Greenland ice sheet in EC-Earth. Cryosphere, 2017, 11, 1949-1965.	3.9	14
53	The PMIP4 contribution to CMIP6 – Part 2: Two interglacials, scientific objective and experimental design for Holocene and Last Interglacial simulations. Geoscientific Model Development, 2017, 10, 3979-4003.	3.6	171
54	The PMIP4 contribution to CMIP6 – Part 3: The last millennium, scientific objective, and experimental design for the PMIP4 <i>past1000</i> simulations. Geoscientific Model Development, 2017, 10, 4005-4033.	3.6	155

QIONG ZHANG

#	Article	IF	CITATIONS
55	Problems encountered when defining Arctic amplification as a ratio. Scientific Reports, 2016, 6, 30469.	3.3	20
56	Impacts of dust reduction on the northward expansion of the African monsoon during the Green Sahara period. Earth and Planetary Science Letters, 2016, 434, 298-307.	4.4	126
57	Arctic climate response to the termination of the African Humid Period. Quaternary Science Reviews, 2015, 125, 91-97.	3.0	27
58	The effect of climate forcing on numerical simulations of the Cordilleran ice sheet at the Last Glacial Maximum. Cryosphere, 2014, 8, 1087-1103.	3.9	24